



Adaptive Under-Frequency Load Shedding Control Strategy of Power Systems With Wind Turbines and UHVDC Participating in Frequency Regulation

Xingyang Wu^{1*}, Feng Xue², Jianfeng Dai³ and Yi Tang⁴

¹College of Energy and Electrical Engineering, Hohai University, Nanjing, China, ²NARI Group Corporation (State Grid Electric Power Research Institute), Nanjing, China, ³College of Automation and College of Artificial Intelligence, Nanjing University of Post and Telecommunication, Nanjing, China, ⁴School of Electrical Engineering, Southeast University, Nanjing, China

OPEN ACCESS

Edited by:

Xiao Wang,
Wuhan University, China

Reviewed by:

Rafael Mihalič,
University of Ljubljana, Slovenia
Jiejie Huang,
Nantong University, China

*Correspondence:

Xingyang Wu
wuxingyang@hhu.edu.cn

Specialty section:

This article was submitted to
Smart Grids,
a section of the journal
Frontiers in Energy Research

Received: 14 February 2022

Accepted: 11 April 2022

Published: 10 May 2022

Citation:

Wu X, Xue F, Dai J and Tang Y (2022)
Adaptive Under-Frequency Load
Shedding Control Strategy of Power
Systems With Wind Turbines and
UHVDC Participating in
Frequency Regulation.
Front. Energy Res. 10:875785.
doi: 10.3389/fenrg.2022.875785

Represented by wind turbines and ultra high-voltage DC (UHVDC), the power-electronic interfaced power sources participate in fast frequency control, which has a significant impact on the power system frequency. However, the conventional under-frequency load shedding (UFLS) scheme doesn't take into account the impact above, resulting in unreasonable load shedding after a large loss of generation. To this end, this article proposes an adaptive UFLS control strategy of power systems with wind turbines and UHVDC participating in frequency regulation. Firstly, based on the virtual inertia control model and the primary frequency control model of wind turbines and UHVDC, the study establishes the simplified frequency response model of the power system considering the participation of wind turbines and UHVDC in frequency regulation. Furthermore, the impact of the active power response characteristics of wind turbines and UHVDC participating in frequency regulation on the magnitude of the active power deficiency is comprehensively analyzed. Thus the precise estimation of the magnitude of the power deficiency can be achieved, which provides technical guidance for multi-stage UFLS. Finally, simulation results demonstrate that the proposed UFLS strategy is capable of reflecting the power system frequency more objectively after a large loss of generation event. In addition, the proposed UFLS strategy outperforms the conventional UFLS strategy in terms of shedding less amount of load when the same desired effect of frequency recovery is achieved.

Keywords: wind turbines, ultra high-voltage DC, under-frequency load shedding, virtual inertia control, primary frequency control, equivalent inertia constant, actual magnitude of power deficiency

INTRODUCTION

The global electric power industry has been in a transition towards low-carbon sustainability in recent years. Conventional synchronous generators will be replaced by large-scale renewable energy sources connected to power systems in the future through power electronic devices (Tian et al., 2021). As a significant part of renewable energy generation, the development of wind power presents a large-scale and high-growth trend. By the end of 2020, the global installed capacity of wind power had reached approximately 743 GW, a 53% growth compared to 2019 [Global Wind Energy Council

(GWEC), 2021]. The gradual replacement of the source-side synchronous generators with power electronic devices intensifies the power-electronization of power systems. Considering the characteristics of the reverse space distribution for renewable energy sources and load centers in some countries and regions, it is imperative to develop long-distance and large-capacity transmission technologies (Pérez-Molina et al., 2020). In China, advanced transmission technologies represented by UHVDC have been applied widely to the promotion of renewable energy consumption and the enhancement of the power supply capacity to load centers. The development of UHVDC transmission accelerates the growth of large-capacity grid-side power electronic devices.

The tendency towards the source- and grid-side power-electronization will dramatically decrease the total system inertia. The frequency stability issues existing in the conventional power systems are becoming more prominent, which is corroborated by incidents such as the blackout in South Australia in September 2016 and the power cut in the U.K. in August 2019 (Australian Energy Market Operator, 2016; National Grid ESO, 2019). To arrest cascading failures and blackouts after a large disturbance occurs in the power grid, UFLS is fully used as the last defense line of the frequency stability control. Generally, we can group all the UFLS schemes into three main categories: conventional UFLS, semi-adaptive UFLS, and adaptive UFLS (Kundur, 2001). In the conventional UFLS schemes, the stages of load shedding, the frequency thresholds of the stages, the time delay, and the load shedding amount are all predefined. Once the frequency drops below the frequency threshold, load shedding is implemented after a certain time delay. The settings of the conventional UFLS schemes derive from assorted presumed power grid parameters including the total system inertia (Horowitz and Phadke, 2008). The time-variant characteristics of the power systems, as well as limited stages and discreteness of load shedding, contribute to the inadaptability of the conventional UFLS schemes to all the system operating conditions. Consequently, it is prone to over- or under-shedding (Sigrist et al., 2012; Rudez and Mihalic, 2016).

To surmount the problems above, numerous scholars have been devoted to the research on semi-adaptive and adaptive UFLS schemes. The load to be shed is determined by the frequency deviation and the rate of change of frequency (RoCoF) in the semi-adaptive UFLS schemes (Anderson and Mirheydar, 1992). In the first stage of load shedding, the amount of load to be shed is calculated based on the swing equation. For the subsequent stages, however, the load shedding amount is predefined. Load shedding is triggered according to the frequency deviation. Hence, semi-adaptive UFLS schemes can not be immune to the problem of inappropriate load shedding. To fill the gap, adaptive UFLS schemes are proposed. The progress of widearea monitoring system (WAMS) technology promotes several adaptive UFLS schemes (Terzija, 2006; Abdelwahid et al., 2014; Tofis et al., 2017). The amount of load shedding is determined by taking advantage of the valuable information provided by WAMS. In addition, numerous scholars pay attention to the thorough and often mathematically complex modification of the entire UFLS (Skrjanc et al., 2021). In

(Hoseinzadeh et al., 2015), a voltage deviation of load buses is used to determine the threshold of each UFLS relay. On the contrary, a continuous UFLS scheme to shed loads in proportion to the frequency deviation is proposed in (Li et al., 2020).

It can be observed from the summarization of the research results that, although massive remarkable work has been done from various angles, there are scarcely any studies on the actual impact of the power-electronic interfaced power sources represented by wind power and UHVDC participating in fast frequency control (Eriksson et al., 2018) on UFLS. In modern power systems, wind turbines mainly use rotor speed control to improve the inertia and primary frequency regulation ability of the system, while variable pitch angle control and matching energy storage system are adopted to improve the rotating reserve capacity of wind farms participating in the system frequency regulation (Vidyanandan and Senroy, 2013; Van de Vyver et al., 2016; Ye et al., 2016; Lyu et al., 2019). In (Li et al., 2017), the impact of virtual inertia response, as well as the characteristics of the under-frequency protection and the power output on the UFLS scheme, are investigated. The UFLS scheme is optimized according to the dynamic calculation of the magnitude of the power deficiency. As one of the main power supplies in the future power grid, wind turbines are required to take the responsibility for frequency regulation by many power systems operators. A UFLS scheme considering the virtual inertia response and the primary frequency control of doubly fed induction generator (DFIG)-based wind turbines is proposed in (Li et al., 2019), which reflects the frequency characteristics of the power grid more objectively. Moreover, the amount of load to be shed in the scheme is less. For UHVDC transmission systems, the characteristics of large transmission capacity and fast power regulation speed make it possible to participate in frequency regulation, which is of great significance to ensure the frequency safety of the power grid. The frequency regulation mechanism, response characteristics, parameter tuning method and limiting factors are quite different from those of wind power generation systems. In (Prakash et al., 2019), an auxiliary frequency control strategy with additional frequency control and automatic generation control for HVDC transmission is presented. In (Ambia et al., 2021), a novel adaptive droop control strategy is proposed to provide power sharing and frequency regulation in HVDC systems. Though the research results above are of great significance in supporting the system frequency stability, none of them makes an attempt to use UHVDC transmission systems to provide inertia support. To address the issue, the coordinated frequency control proposed in (Shi et al., 2021) is realized by introducing the virtual inertia control on the basis of the frequency droop control.

From the analysis above, it is obvious that the participation of wind turbines and UHVDC in frequency regulation shows a great favorable influence on the frequency characteristics of the power grid. However, none of the existing UFLS schemes take into account the actual effect of frequency regulation with the participation of wind turbines and UHVDC. On one hand, the virtual inertia response of wind turbines and UHVDC leads to the alteration of the equivalent inertia of the power grid, further influencing the calculation of the magnitude of the power

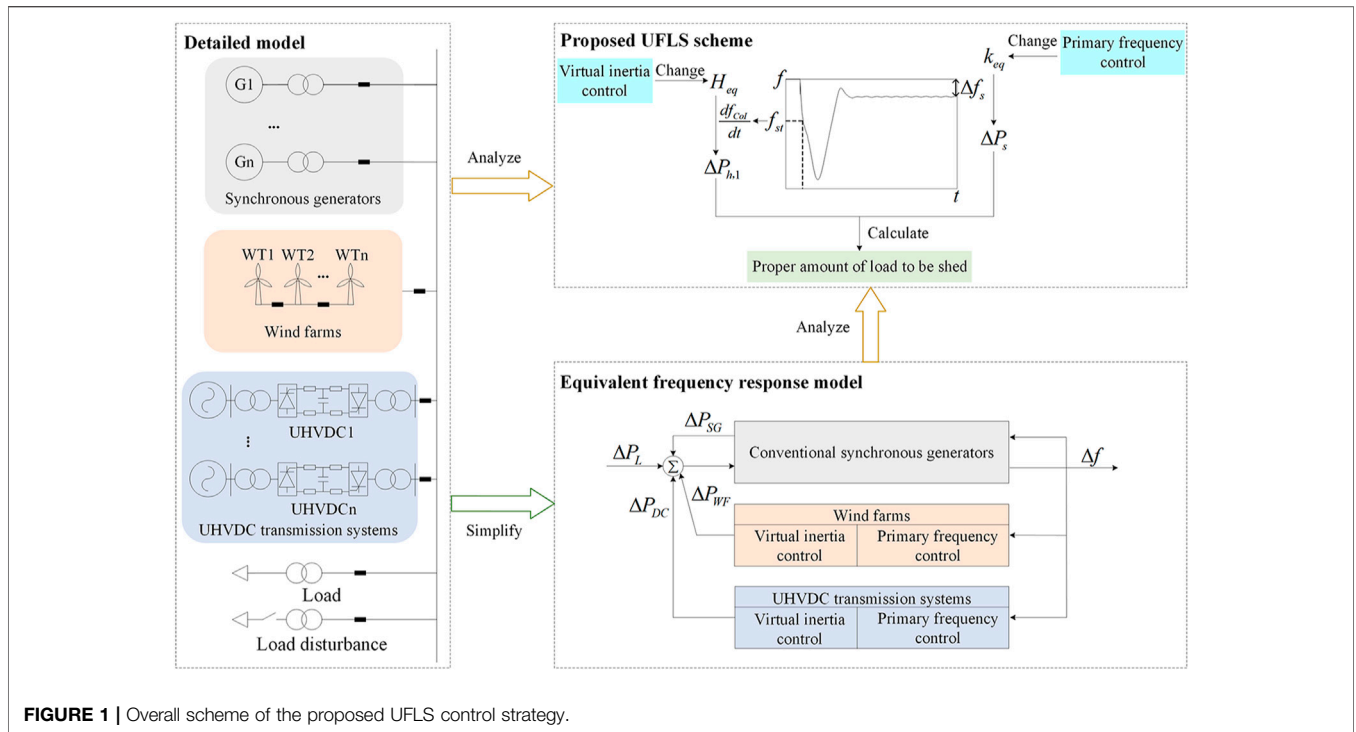


FIGURE 1 | Overall scheme of the proposed UFLS control strategy.

deficiency. On the other hand, the primary frequency control of wind turbines and UHVDC can offset the power deficiency. Ignoring the offset will bring about the problems of over-shedding and economic loss. Therefore, the existing UFLS schemes are not applicable to the modern power system with wind turbines and UHVDC participating in frequency regulation. It is urgent to solve the issue for the sake of the frequency safety of the power grid.

This article proposes an adaptive UFLS control strategy of the power system with wind turbines and UHVDC participating in frequency regulation. Firstly, based on the virtual inertia control model and the primary frequency control model, we establish the simplified frequency response model of the power system considering the participation of wind turbines and UHVDC in frequency regulation. Then the impact of the active power response characteristics of wind turbines and UHVDC participating in frequency regulation on the magnitude of the power deficiency is comprehensively analyzed. Afterward, in light of the estimation result of the magnitude of the power deficiency, the amount of load to be shed in the multi-stage UFLS scheme is determined. Finally, simulation results are presented and discussed to illustrate the outperformance of the proposed UFLS control strategy.

OVERALL SCHEME OF THE PROPOSED UNDER-FREQUENCY LOAD SHEDDING CONTROL STRATEGY

After the integration of a high proportion of wind power and UHVDC, wind turbines and UHVDC participate in frequency

regulation by means of virtual inertia control and primary frequency control. However, the existing UFLS schemes do not take into account the situation, which possibly causes frequency trajectory distortion and unreasonable load shedding. To address the issue, this paper proposes an adaptive UFLS control strategy of power systems with wind turbines and UHVDC participating in frequency regulation. The overall scheme of the strategy is shown in **Figure 1**.

It can be seen from **Figure 1** that, this paper firstly simplifies the detailed models of synchronous generators, wind turbines, UHVDC and load. Afterward, the equivalent frequency response model of the power system considering the virtual inertia control and the primary frequency control of the wind turbines and UHVDC is obtained. Based on the detailed models and the equivalent frequency response model, this paper analyzes the two main effects which are brought about by the integration of large-scale wind power and UHVDC on the power grid. For one thing, the virtual inertia control of the wind turbines and UHVDC changes the equivalent inertia constant of the power grid H_{eq} , thus influencing the calculation result of the magnitude of the power deficiency $\Delta P_{h,1}$ when the system frequency reaches the frequency threshold of the first stage f_{st} . For another, after the primary frequency control of the wind turbines and UHVDC is taken into account, ΔP_s refers to the active power provided not only by the primary frequency response of the synchronous generators and the effect of load regulation, but also the primary frequency response of the wind turbines and UHVDC. This impact is reflected in the equivalent power regulation coefficient k_{eq} . This coefficient k_{eq} includes the unit power regulation of the synchronous generators and the load, as well as the droop control gain of the wind turbines and UHVDC

participating in primary frequency control. Thus ΔP_s needs to be revised when compared to the situation without considering the primary frequency control of the wind turbines and UHVDC. Finally, this paper precisely calculate the amount of load to be shed of UFLS based on $\Delta P_{h,1}$ and ΔP_s to achieve the frequency recovery of the power system.

CONTROL MODELS OF WIND TURBINES AND ULTRA HIGH-VOLTAGE DC PARTICIPATING IN FREQUENCY REGULATION

Control Model of Wind Turbines Participating in Frequency Regulation

Taking DFIG-based wind turbines as an example, the control model of the wind turbines participating in frequency regulation is analyzed and established considering the virtual inertia control and the primary frequency control.

DFIG-based wind turbines lack intrinsic inertia from the system aspect for the reason that their mechanical rotor speed is decoupled with system frequency. However, by introducing an auxiliary virtual inertia control loop in the maximum power tracking loop of the DFIG rotor-side convertor, the wind turbines can also supply the power grid with the virtual inertia response. The rate of change of frequency, i.e. df/dt , is the input of the virtual inertia control. The system frequency drops when the power grid suffers a power deficiency. The virtual inertia control shares part of the power deficiency by rapidly augmenting the active power output of the wind turbines. The active power increment ΔP_{inWF} comes from the released kinetic energy, as expressed in Eq. 1. It is conducive to alleviating the sudden change in the frequency of the power grid. The virtual inertia control provides the wind turbines with the ability to support the total system inertia.

$$\Delta P_{inWF} = -k_{inWF} \frac{df}{dt} \quad (1)$$

Where k_{inWF} is the inertia time constant of the wind turbines; f is the system frequency.

Similar to the droop control of synchronous generators, the primary frequency control of the wind turbines is designed in this study. The frequency deviation, i.e. $f - f_{nom}$, is the input of the primary frequency control. When the system frequency drops due to the power deficiency, the active power increment provided by the wind turbines can be expressed as

$$\Delta P_{dWF} = -k_{dWF} (f - f_{nom}) \quad (2)$$

Where k_{dWF} is the droop control gain of the wind turbines participating in the primary frequency control; f_{nom} is the system nominal frequency.

The control model of the wind turbines participating in frequency regulation combines the virtual inertia control and the primary frequency control holistically. Figure 2 shows the control block diagram.

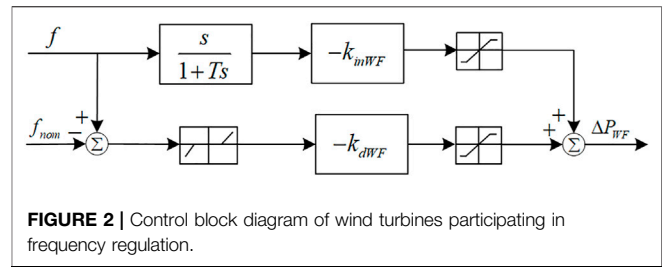


FIGURE 2 | Control block diagram of wind turbines participating in frequency regulation.

In Figure 2, T is filter time constant; ΔP_{WF} is the active power increment provided by the control model of wind turbines participating in frequency regulation, as expressed in Eq. 3.

$$\Delta P_{WF} = -k_{dWF} (f - f_{nom}) - k_{inWF} \frac{df}{dt} \quad (3)$$

Control Model of Ultra High-Voltage DC Participating in Frequency Regulation

At present, the participation of UHVDC transmission systems in frequency regulation mainly includes two frequency control modes based on the PI controller and the droop controller, respectively. In this article, the frequency control mode based on the droop controller is used as the primary frequency control of UHVDC. The control block diagram is shown in Figure 3.

In Figure 3, T_1 and T_2 are filter time constants; k_{dDC} is the proportional coefficient of UHVDC; ΔP_{dDC} is the active power increment of UHVDC participating in primary frequency control.

By introducing the virtual inertia control on the basis of the regular droop control, UHVDC is capable of participating in the process of the system inertia response. It helps to reduce the rate and range of the frequency deviation when the power grid suffers a huge power deficiency. The active power increment ΔP_{DC} provided by UHVDC participating in frequency regulation can be expressed as follows:

$$\Delta P_{DC} = -k_{dDC} (f - f_{nom}) - k_{inDC} \frac{df}{dt} \quad (4)$$

Where k_{inDC} is the differential coefficient of UHVDC.

Similar to the control model of wind turbines participating in frequency regulation established in Section 3.1, the droop control of UHVDC is mainly in response to the frequency deviation, while the virtual inertia control of UHVDC is mainly in response to the frequency differential quantity. Thus UHVDC can simultaneously participate in the process of the inertia response and the primary frequency control, the same as synchronous generators.

As shown in Figure 4, typical HVDC transmission system mainly consists of rectifier station, DC transmission line and inverter station. In this paper, the virtual inertia control and the primary frequency control of UHVDC can be realized by modifying the UHVDC control systems. P_{DC-ref} is the active power reference value of UHVDC, and P_{DC} is the active power

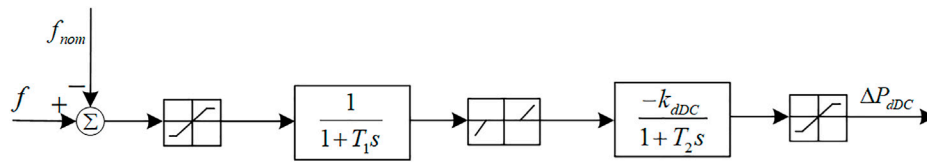


FIGURE 3 | Block diagram of the primary frequency control base on the droop controller of UHVDC.

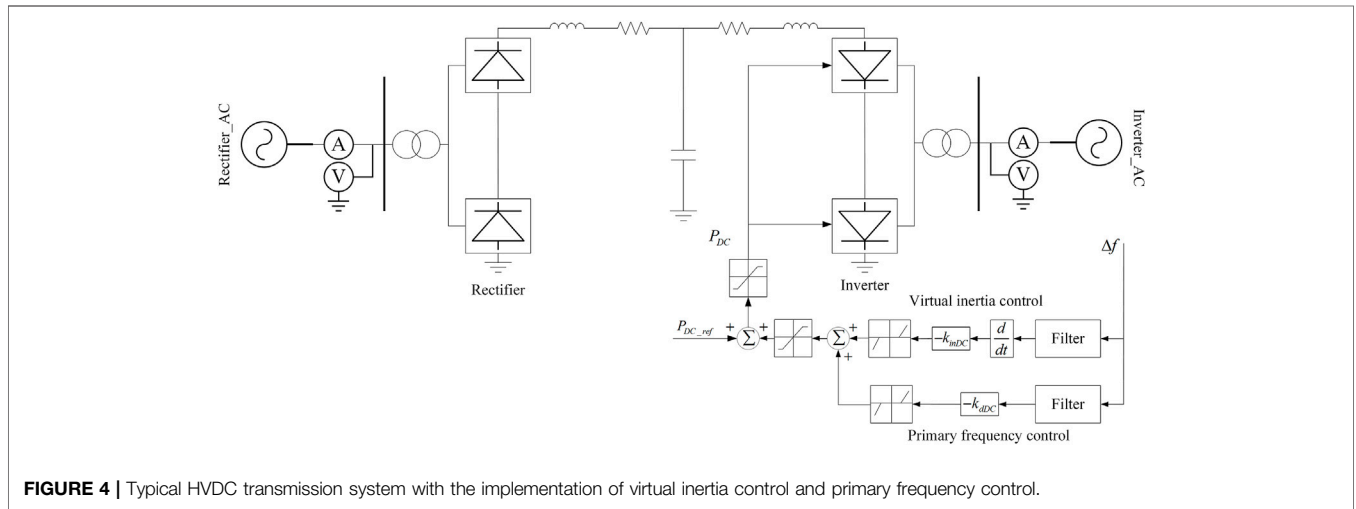


FIGURE 4 | Typical HVDC transmission system with the implementation of virtual inertia control and primary frequency control.

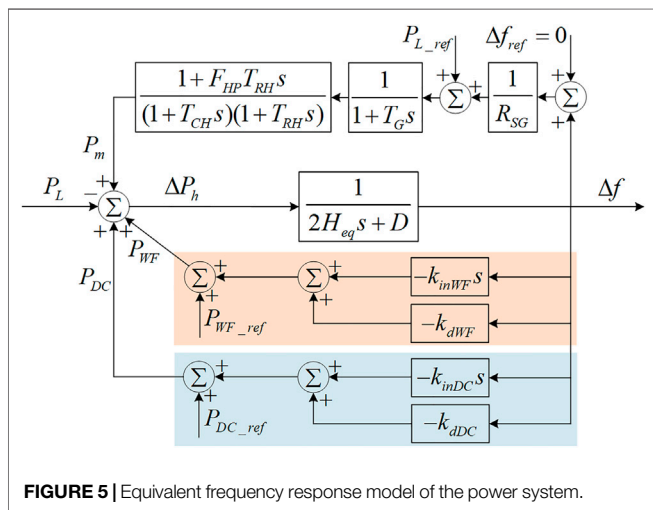


FIGURE 5 | Equivalent frequency response model of the power system.

which needs to be provided by UHVDC. Δf is the system frequency deviation.

The power regulation of UHVDC systems is rapid enough to ensure that the response time is no longer than 150 ms after a power step disturbance occurs. The frequency regulation process of the power system belongs to the electromechanical transient process, of which the timescale is usually second level. Therefore, the regulation process of the UHVDC systems can be neglected in the process of analyzing the UHVDC frequency regulation

mechanism, and the UHVDC transmission power strictly tracks the reference command. In addition, the effects of the filtering link, the deadband link, and the power amplitude limiting link are further neglected to simplify the analyzing process.

Based on the analysis above, the equivalent frequency response model of the power system including the virtual inertia control and the primary frequency control of wind turbines and UHVDC is shown in **Figure 5**. Where Δf_{ref} is the system frequency deviation reference value; P_{L_ref} is the load power reference value; R_{SG} is the equivalent droop parameter of the power grid; T_G is the main servo time constant; T_{CH} is the time constant of main inlet volumes and steam chest; T_{RH} is the time constant of reheater; F_{HP} is the fraction of total turbine power generated by high pressure (HP) sections; H_{eq} and D are the inertia constant and the damping coefficient of the equivalent generator of the power grid, respectively; P_m is the mechanical power provided by the synchronous generators in the power grid; P_L is the load power of the power grid; P_{WF_ref} and P_{DC_ref} are the active power reference value of wind power and UHVDC, respectively; P_{WF} and P_{DC} are the active power provided by wind power and UHVDC, respectively; ΔP_h is the actual magnitude of the active power deficiency.

Assume that a sudden increase of load occurs and results in a power deficiency ΔP_{de} . Based on **Figure 5**, the equivalent rotor motion equation of the power system (transferred into the time domain equation) can be represented as

$$2H_{eq} \frac{d\Delta f}{dt} = P_{m0} + \Delta P_m + \Delta P_{WF} + \Delta P_{DC} - P_{e0} - D\Delta f - \Delta P_{de} \quad (5)$$

where P_{m0} and P_{e0} are the initial mechanical power and electromagnetic power of the power system, respectively; ΔP_m is the mechanical power increment provided by the synchronous generators; ΔP_{WF} and ΔP_{DC} are the power increment provided by the wind power and UHVDC, separately.

ADAPTIVE UNDER-FREQUENCY LOAD SHEDDING CONTROL STRATEGY OF POWER SYSTEMS WITH WIND TURBINES AND ULTRA HIGH-VOLTAGE DC PARTICIPATING IN FREQUENCY REGULATION

The participation of the wind turbines and UHVDC in frequency regulation of the power system affects UFLS mainly from two aspects as follows: 1) The virtual inertia control provides the wind turbines and UHVDC with virtual inertia and changes the equivalent inertia of the power grid, thus influencing the calculation of the magnitude of the power deficiency. 2) The primary frequency control of the wind turbines and UHVDC offsets part of the magnitude of the power deficiency corresponding to the steady-state frequency deviation, which contributes to less amount of load to be shed. In conclusion, both the virtual inertia control and the primary frequency control influence the calculation result of the total amount of load to be shed in the UFLS scheme.

Dynamic Calculation of the Magnitude of the Power Deficiency

When we study the frequency characteristics of the power system integrated with wind power and UHVDC, one of the difficult problems we face with is the calculation of the system equivalent inertia constant H_{eq} . For most situations, the inertia constant of the synchronous generators is a definite number. However, it is hard to analyze and calculate the equivalent inertia constants of the wind turbines and UHVDC. In the adaptive UFLS schemes, the actual magnitude of the power deficiency is commonly calculated as follows

$$\Delta P_h = \frac{2H_{eq}}{f_{nom}} \frac{df_{CoI}}{dt} \quad (6)$$

It is obvious from Eq. 6 that we can calculate H_{eq} precisely after we obtain the power disturbance variation ΔP around the time when the operating status of the power system changes or the disturbance occurs, as well as the RoCoF of CoI $\frac{df_{CoI}}{dt}$, as expressed in Eq. 7.

$$H_{eq} = \frac{\Delta P f_{nom}}{2 \frac{df_{CoI}}{dt}} \quad (7)$$

Furthermore, in order to reduce the error of calculating the equivalent inertia constant H_{eq} , the study employs the method as follows: by maintaining the current operating state of the power system unchanged and setting L different and known power disturbance variation $\Delta P_{set,l}$, the corresponding RoCoF of CoI $\frac{df_{CoI}}{dt}$ can be calculated. Solve all the values of the equivalent inertia constant $H_{eq,l}$ corresponding to $\Delta P_{set,l}$ according to Eq. 7. Then calculate the mean value of $H_{eq,l}$ as the setting value of the equivalent inertia constant of the power system, which can be represented as

$$H_{eq} = \frac{\sum_{l=1}^L H_{eq,l}}{L} = \frac{\sum_{l=1}^L \Delta P_{set,l} f_{nom}}{2L \frac{df_{CoI}}{dt}} \quad (8)$$

After the system equivalent inertia constant H_{eq} is obtained, calculate the actual magnitude of the power deficiency $\Delta P_{h,1}$ at the time when the system frequency drops to the frequency threshold in the first stage of UFLS.

Assume that the steady-state frequency after UFLS is f_s . As $f_s < f_{nom}$, the steady-state frequency deviation is $\Delta f_s = f_s - f_{nom}$. Considering the participation of the wind turbines and UHVDC in primary frequency control, ΔP_s refers to the active power provided by the primary frequency control of the synchronous generators, the wind turbines, and UHVDC, together with the effect of load regulation, as expressed in Eq. 8.

$$\Delta P_s = -(k_L + k_G + k_{dWF} + k_{dDC}) \Delta f_s \quad (9)$$

where k_L and k_G are the unit regulation power of the load and the synchronous generators, respectively.

Then the total amount of load to be shed $P_{shed,\Sigma}$ can be calculated as (Yang, 2007)

$$\Delta P_{shed,\Sigma} = \frac{\Delta P_{h,1} - (k_L + k_G + k_{dWF} + k_{dDC}) P_{L_s} \Delta f_s^*}{1 - (k_L + k_G + k_{dWF} + k_{dDC}) \Delta f_s^*} \quad (10)$$

where P_{L_s} is the load of the power grid in the steady state; Δf_s^* is the per unit steady-state frequency deviation.

Then the total amount of the load will be shed by stages. It is obvious from Eq. 9 that the primary frequency control of the wind turbines and UHVDC leads to the increase in their active power output in steady state, thus reducing $\Delta P_{h,1}$.

Implementation Strategy of Under-Frequency Load Shedding

Firstly, determine the stages, frequency thresholds, load shedding percentage in each stage, and steady-state recovery frequency in the UFLS control strategy.

In the process of UFLS, the first frequency threshold should not exceed 49.25 Hz to fully use the rotating reserve capacity of the power system. The typical frequency difference between the stages is 0.2~0.25 Hz and 5~8 stages are commonly set. Based on the UFLS schemes of actual power grids, this paper sets four basic stages with the corresponding frequency thresholds of 49.2, 49.0, 48.8, 48.6 Hz, and the time delay of 0.2 s. The load shedding percentages in the basic stages are 20, 25, 25, and 30%, separately.

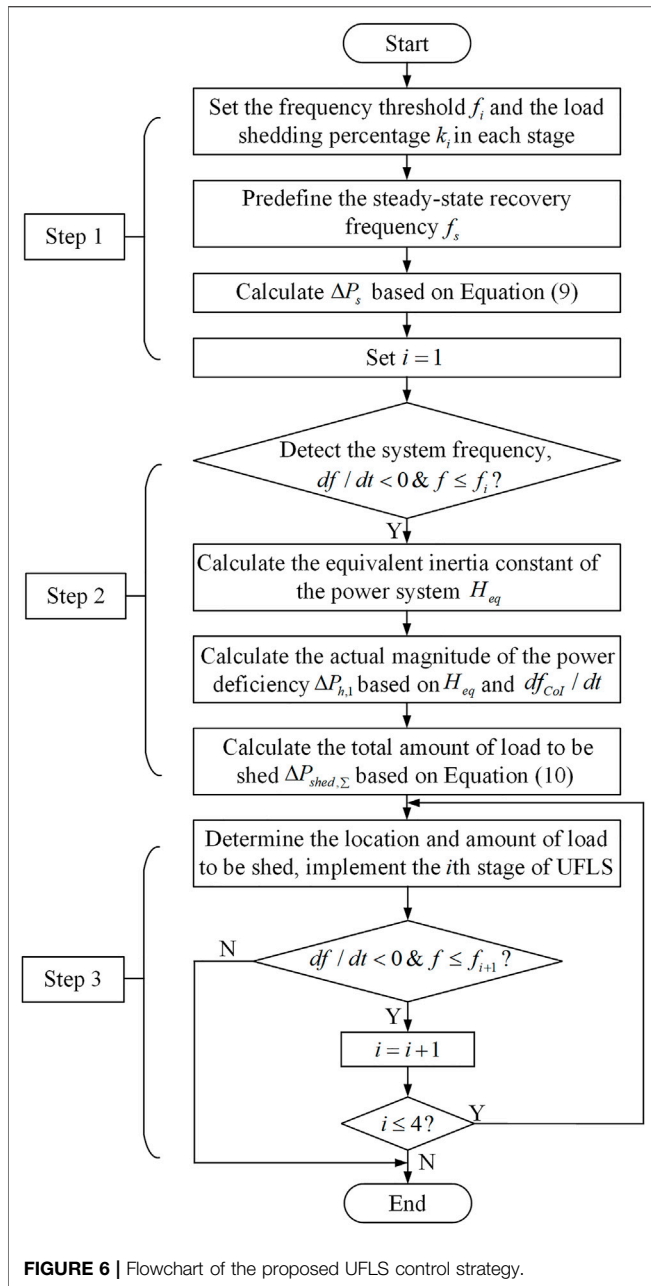


FIGURE 6 | Flowchart of the proposed UFLS control strategy.

Afterward, determine the location and the amount of load to be shed in the UFLS control strategy.

In the actual operation of UFLS, the load of the scattered nodes needs to be shed. The load shedding location can be selected and the load shedding amount can be allocated based on the load shedding sensitivity index (Yang and Cai, 2016). The load shedding amount of the n th node of the power grid $\Delta P_{shed,n}$ can be determined as

$$\Delta P_{shed,n} = \frac{\Delta P_{shed,i} \phi_n}{\sum_{n=1}^N \phi_n} \quad (11)$$

where $\Delta P_{shed,i}$ is the total amount of load to be shed in the i th stage; ϕ_n is the load shedding sensitivity of the load node, directly related to the electrical distance from the load node to the disturbance node; N is the total number of the load nodes.

Finally, design the UFLS implementation strategy.

In this study, the UFLS control strategy is implemented as shown in Figure 6. The corresponding steps can be described as follows:

- 1) Set the frequency threshold f_i and the load shedding percentage k_i in each stage. Predefine the steady-state recovery frequency f_s . Calculate ΔP_s according to Eq. 9. Set $i = 1$.
- 2) Detect the frequency state of the power system. If $\frac{df}{dt} < 0$ and $f \leq f_i$, then calculate the equivalent inertia constant of the power system H_{eq} by using the method proposed in Section 4.1. Then based on H_{eq} and $\frac{df_{col}}{dt}$, the actual magnitude of the power deficiency at the time when the system frequency drops to the first frequency threshold $\Delta P_{h,1}$ can be obtained according to Eq. 6.
- 3) On the basis of $\Delta P_{h,1}$ and Eq. 10, calculate the total amount of load to be shed $\Delta P_{shed,\Sigma}$ in the UFLS control strategy.

It can be seen from Figure 6 that when the system frequency reaches the threshold of the i th stage, i.e. $f \leq f_i$, UFLS is started in accordance with the load shedding percentage in each stage k_i . After completing load shedding in the i th stage, detect the system frequency. If $\frac{df}{dt} < 0$ and $f \leq f_{i+1}$, it is clear that the load shedding amount is not enough to avoid the frequency from declining. Then the next stage of UFLS is triggered. Conversely, it means that load shedding has already restrained the descending of the system frequency. The frequency does not fall below the frequency threshold in the $(i + 1)$ th stage. The UFLS process ends.

SIMULATION ANALYSIS

In this section, simulations are carried out on the IEEE 39-bus test system. Power System Analysis Synthesis Program (PSASP) developed by China Electric Power Research Institute is used to conduct the simulation studies. The single-line diagram of this test system is provided in Figure 7. Suppose that DFIG-based wind turbines are connected at Bus 34 and Bus 36 replacing the thermal generators with equal active power output. A UHVDC transmission line with a rated active power output of 1000 MW is connected to the system at Bus 18, replacing the thermal generators at Bus 30 and Bus 32. To achieve the power equilibrium, we also reduce the active power output of the thermal generator at Bus 31. Both the wind turbines and UHVDC have the abilities of virtual inertia control and primary frequency control. We set the available capacity of the wind turbines for frequency regulation as 10% of their rated active power (Lyu et al., 2021). The available capacity of UHVDC for frequency regulation is set as 5% of its rated active power (Zhao, 2004).

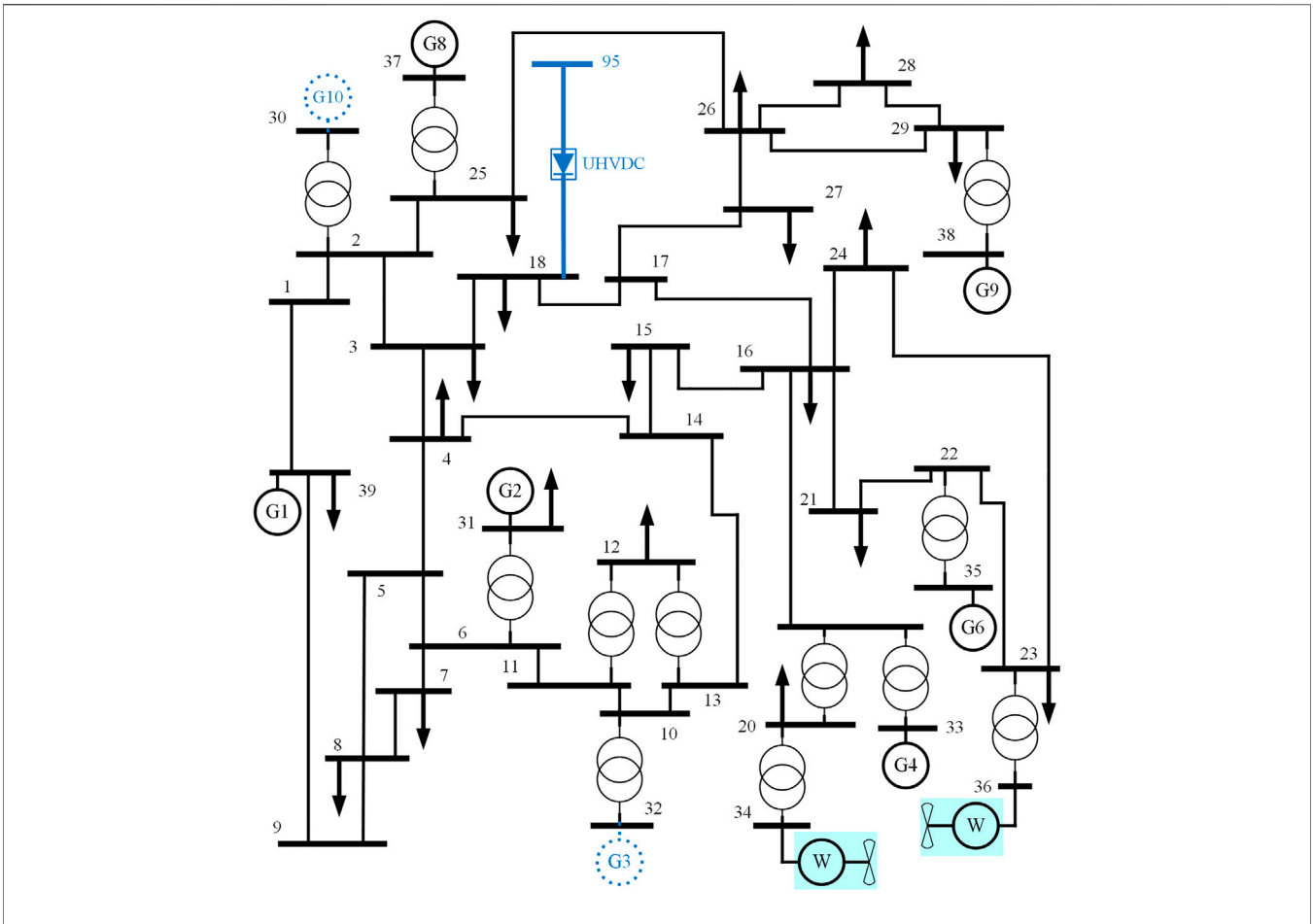


FIGURE 7 | Single-line diagram of the IEEE 39-bus test system with wind turbines and UHVDC.

Impact of Wind Turbines and Ultra High-Voltage DC Participating in Frequency Regulation on Frequency Response

In this case, when $t = 5\text{ s}$, a 300 MW load surge at Bus 21 occurs. This disturbance is used to imitate the power deficiency caused by new energy or conventional generators off-grid. Simulate and compare the effects of four frequency control modes on the system frequency response after the disturbance: 1) both the wind turbines and UHVDC participate in frequency regulation; 2) only the wind turbines participate in frequency regulation; 3) only UHVDC participates in frequency regulation; 4) neither the wind turbines nor UHVDC participates in frequency regulation. The simulation results are shown in Figure 8.

It is revealed from Figure 8 that when neither the wind turbines nor UHVDC participates in frequency regulation, the maximum frequency deviation is the largest and the steady-state frequency is the lowest of the four frequency control modes. Besides, the frequency nadir drops below 49.2 Hz, violating the frequency threshold of the first stage. Once the wind turbines or UHVDC participates in frequency regulation, the absolute maximum frequency deviation decreases by 0.4 Hz, and the steady-state frequency is higher. When both the wind turbines

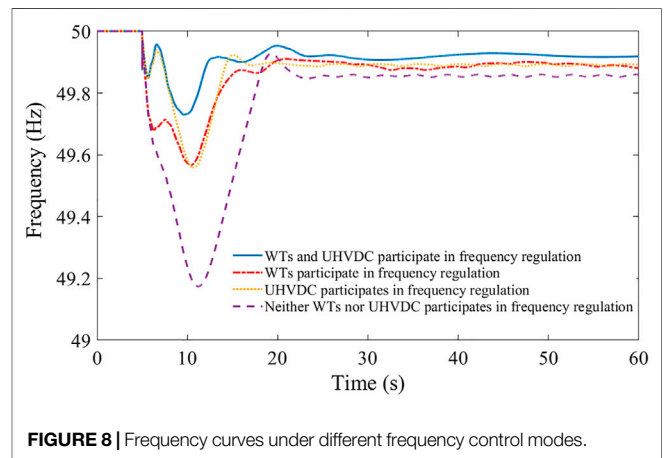


FIGURE 8 | Frequency curves under different frequency control modes.

and UHVDC participate in frequency regulation, the maximum frequency deviation and the steady-state frequency deviation are the minima. It can be inferred that the participation of the wind turbines and UHVDC in frequency regulation can effectively ameliorate the system frequency characteristics. The combined

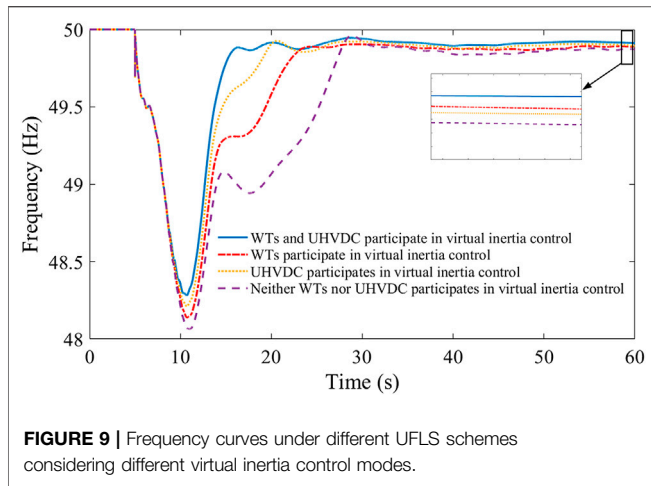


FIGURE 9 | Frequency curves under different UFLS schemes considering different virtual inertia control modes.

action of the virtual inertia control and the primary frequency control significantly decreases the maximum frequency deviation and the steady-state frequency deviation. Thus the dynamic process and the trajectory of the system frequency are notably impacted by the participation of the wind turbines and UHVDC in frequency regulation.

Impact of Virtual Inertia Control of Wind Turbines and Ultra High-Voltage DC on Under-Frequency Load Shedding

For cases in Sections 5.2, 5.3, and 5.4, a 780 MW load surge at Bus 21 at the time $t = 5$ s is used as the disturbance to imitate the power deficiency caused by new energy or conventional generators off-grid.

In this case, both the wind turbines and UHVDC in the test system possess the capability of virtual inertia control actually. However, to illustrate the impact of the virtual inertia control of the wind turbines and UHVDC on UFLS, we consider four different situations in the process of formulating four UFLS schemes respectively: 1) both the wind turbines and UHVDC participate in virtual inertia control; 2) only the wind turbines participate in virtual inertia control; 3) only UHVDC participates in virtual inertia control; 4) neither the wind turbines nor UHVDC participates in virtual inertia control. Then the four UFLS schemes are implemented on the same test system in which both the wind turbines and UHVDC participate in virtual inertia control, separately. The simulation results are shown in Figure 9 and Table 1.

It can be seen from Figure 9 and Table 1 that, the steady-state recovery frequency in scheme 1 is the highest, followed by scheme 3 and scheme 2, while in scheme 4 is the lowest. The reason is that for one thing, the virtual inertia control of the wind turbines and UHVDC is considered in scheme 1 so that the calculated inertia constant H_{eq} is the largest. However, scheme 2 only accounts for the virtual inertia control of the wind turbines, and scheme 3 only takes the virtual inertia control of UHVDC into account. Thus the calculated H_{eq} in scheme 2 and scheme 3 is less. As scheme 4 does not consider

TABLE 1 | Results of different UFLS schemes considering different virtual inertia control modes.

UFLS scheme	Steady-state frequency (Hz)	Load shedding amount (MW)
1	49.9127	560
2	49.8860	482
3	49.8941	519
4	49.8713	437

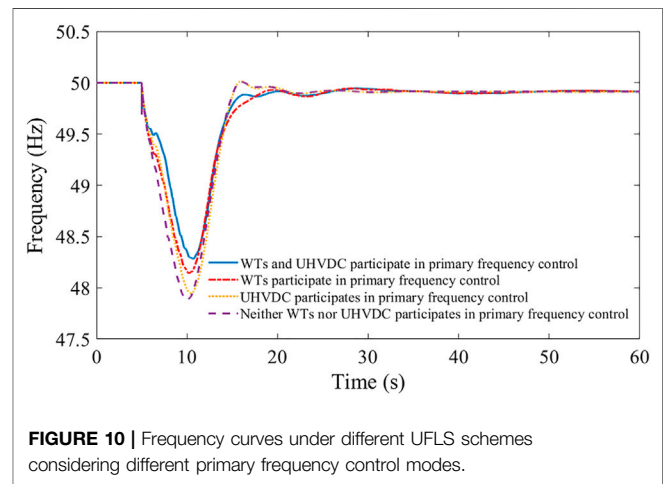


FIGURE 10 | Frequency curves under different UFLS schemes considering different primary frequency control modes.

the virtual inertia control of the wind turbines or UHVDC, the calculated H_{eq} in scheme 4 is the least. For another, it can be inferred from Eq. 10 that the further calculated total amount of load to be shed $\Delta P_{shed, \Sigma}$ is the largest in scheme 1, followed by scheme 3 and scheme 2, while in scheme 4 is the least. Thus the steady-state recovery frequency in each scheme has certain differences.

The simulation results in this case also demonstrate that when the virtual inertia control of the wind turbines and UHVDC is taken into consideration, scheme 1 can calculate the actual magnitude of the power deficiency more precisely and reflect the effect of the virtual inertia control on UFLS more objectively. Obviously, the effect is significant.

Impact of Primary Frequency Control of Wind Turbines and Ultra High-Voltage DC on Under-Frequency Load Shedding

In this case, to illustrate the impact of the primary frequency control of the wind turbines and UHVDC on UFLS, design and contrast four different UFLS schemes: 1) UFLS scheme considering the primary frequency control of both the wind turbines and UHVDC; 2) UFLS scheme only considering the primary frequency control of the wind turbines; 3) UFLS scheme only considering the primary frequency control of UHVDC; 4) UFLS scheme without considering the primary frequency control of wind turbines or UHVDC. Then each of the four schemes is implemented on the test system with the primary frequency

TABLE 2 | Results of different UFLS schemes considering different primary frequency control modes.

UFLS scheme	Steady-state frequency (Hz)	Load shedding amount (MW)
1	49.9127	560
2	49.9127	633
3	49.9120	628
4	49.9133	704

control mode corresponding to the scheme itself. The simulation results are shown in **Figure 10** and **Table 2**.

It can be observed from **Figure 10** and **Table 2** that, the steady-state recovery frequency is almost the same in the four schemes. However, the amount of load to be shed $\Delta P_{shed, \Sigma}$ in scheme 1 is 560 MW, which is 73 MW, 68 MW, and 144 MW less than that in scheme 2, scheme 3, and scheme 4, respectively. This shows that the magnitude of the power deficiency is partly offset by the primary frequency control of the wind turbines and UHVDC in scheme1, resulting in the decrease in the amount of load to be shed by 144 MW compared with scheme 4. Schemes 2 and scheme 3 respectively take into account the primary frequency control of wind turbines and UHVDC. The part of the magnitude of the power deficiency offset by the primary frequency control is less than that in scheme 1. Thus the amount of load to be shed in scheme 2 and scheme 3 is more than that in scheme 1. As neither the primary frequency control of the wind turbines nor of UHVDC is taken into account in scheme 4, more load needs to be shed to maintain the same steady-state recovery frequency as that in scheme 1, scheme 2, and scheme 3. To conclude, the primary frequency control of the wind turbines and UHVDC has a prominent effect on the steady-state recovery results and the amount of load to be shed.

Verification of Adaptive Under-Frequency Load Shedding Control Strategy With Wind Turbines and Ultra High-Voltage DC Participating in Frequency Regulation

In this case, simulations are conducted to compare three different UFLS schemes. Scheme 1 is the scheme proposed in this paper, which is performed according to the implementation strategy of UFLS in **Figure 5**. Scheme 2 is the conventional UFLS scheme in literature (Rudez and Mihalic, 2011). Scheme 3 is the adaptive UFLS scheme in literature (Song et al., 2014) without considering the virtual inertia control and the primary frequency control of the wind turbines and UHVDC. Compare the frequency response curves and the steady-state results of all the schemes in the process of UFLS. The simulation results are shown in **Figure 11** and **Table 3**.

It can be seen from **Figure 11** and **Table 3** that all the schemes complete the action process of UFLS through four stages of load shedding, and the steady-state recovery frequency is close. However, the load shedding amount in scheme 1 is evidently less than that in scheme 2 and scheme 3 in each stage

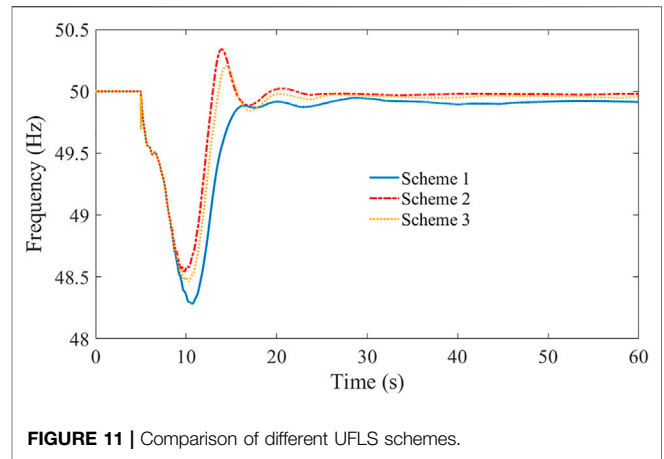


FIGURE 11 | Comparison of different UFLS schemes.

TABLE 3 | Load shedding amount and steady-state frequency of different UFLS schemes.

Load shedding stages	Load shedding amount (MW)		
	Scheme 1	Scheme 2	Scheme 3
First stage	112	156.2	137.6
Second stage	140	195.25	172
Third stage	140	195.25	172
Fourth Stage	168	234.3	206.4
Total	560	781	688
Steady-state frequency (Hz)	49.9127	49.9781	49.9552

and in total. The reasons for the difference in the load shedding amount are as follows. On one hand, the actual magnitude of the power deficiency $\Delta P_{h,1}$ is calculated in scheme 1 considering the virtual inertia control and the primary frequency control of the wind turbines and UHVDC. On the other hand, the total amount of load to be shed $\Delta P_{shed, \Sigma}$ is calculated in scheme 1 considering the primary frequency control of the wind turbines and UHVDC. Thus the simulation results show that when taking into account the virtual inertia control and the primary frequency control of the wind turbines and UHVDC, the load shedding amount can be significantly reduced on the premise of reaching the steady-state recovery frequency. Thus it is conducive to the improvement of the power supply reliability of the power grid and the reduction of the loss caused by load shedding.

CONCLUSION

This paper proposes an adaptive UFLS control strategy of power systems with wind turbines and UHVDC participating in frequency regulation. The following conclusions are obtained through theoretical research and simulation verification.

- 1) The virtual inertia control of the wind power and UHVDC has a significant impact on the frequency dynamic process and trajectory, resulting in the obvious differences in the

calculation results of the magnitude of the power deficiency and the amount of load to be shed, which makes the steady-state recovery frequency higher.

- 2) The primary frequency control of the wind power and UHVDC can effectively offset part of the power deficiency magnitude and reduce the load shedding amount.
- 3) Compared with the existing typical UFLS strategies, on the premise of reaching the same level of steady-state recovery frequency, the strategy proposed in this paper can shed the least amount of load. Moreover, it can better adapt to the UFLS process of the power grid with the wind turbines and UHVDC participating in frequency regulation.

This paper takes DFIG-based wind turbines and UHVDC as examples to discuss the UFLS control strategy. In the future, we will further study other UFLS improvement strategies considering frequency regulation of other types of renewable energy, flexible DC, and energy storage, so as to provide a better guarantee for the safety and stability of the power grid frequency.

REFERENCES

- Abdelwahid, S., Babiker, A., Eltom, A., and Kobet, G. (2014). Hardware Implementation of an Automatic Adaptive Centralized Underfrequency Load Shedding Scheme. *IEEE Trans. Power Deliv.* 29 (6), 2664–2673. doi:10.1109/TPWRD.2014.2331495
- Ambia, M. N., Meng, K., Xiao, W., Al-Durra, A., and Dong, Z. Y. (2021). Adaptive Droop Control of Multi-Terminal HVDC Network for Frequency Regulation and Power Sharing. *IEEE Trans. Power Syst.* 36 (1), 566–578. doi:10.1109/TPWRS.2020.2999443
- Anderson, P. M., and Mirheydar, M. (1992). An Adaptive Method for Setting Underfrequency Load Shedding Relays. *IEEE Trans. Power Syst.* 7 (2), 647–655. doi:10.1109/59.141770
- Australian Energy Market Operator (2016). *Black System South Australia 28 September 2016—Third Preliminary Report*. Australia: Australian Energy Market Operator Limited.
- Eriksson, R., Modig, N., and Elkington, K. (2018). Synthetic Inertia versus Fast Frequency Response: A Definition. *IET Renew. Power Generation* 12 (5), 507–514. doi:10.1049/iet-rpg.2017.0370
- Global Wind Energy Council (GWEC) (2021). *Global Wind Report 2021*. Brussels, Belgium: Global Wind Energy Council.
- Horowitz, S. H., and Phadke, A. G. (2008). *Power System Relaying*. Hoboken, NJ, USA: Wiley.
- Hoseinzadeh, B., da Silva, F. M. F., and Bak, C. L. (2015). Adaptive Tuning of Frequency Thresholds Using Voltage Drop Data in Decentralized Load Shedding. *IEEE Trans. Power Syst.* 30 (4), 2055–2062. doi:10.1109/TPWRS.2014.2351015
- Kundur, P. (2001). *Power System Stability and Control*. Beijing: China Electric Power Press.
- Li, C., Wu, Y., Sun, Y., Zhang, H., Liu, Y., Liu, Y., et al. (2020). Continuous Underfrequency Load Shedding Scheme for Power System Adaptive Frequency Control. *IEEE Trans. Power Syst.* 35 (2), 950–961. doi:10.1109/TPWRS.2019.2943150
- Li, S. C., Lyu, X. S., Zhong, H., Long, Q. W., Xie, W. J., and Shu, Z. Y. (2019). Adaptive Under-frequency Load Shedding Strategy of Power Grid with Large-Scale DFIG Wind Turbines Participating in Frequency Regulation. *Automation Electric Power Syst.* 43 (15), 109–120. doi:10.7500/AEPS2018112800
- Li, S., Liao, Q. F., Tang, F., Zhao, H. S., and Shao, Y. G. (2017). Adaptive Underfrequency Load Shedding Strategy Considering High Wind Power Penetration. *Power Syst. Tech.* 41 (4), 1084–1090. doi:10.13335/j.1000-3673.pst.2016.3029

DATA AVAILABILITY STATEMENT

The original contributions presented in the study are included in the article/**Supplementary Material**, further inquiries can be directed to the corresponding author.

AUTHOR CONTRIBUTIONS

XW: Methodology, Software, Validation, Investigation, Data curation, Writing—original draft preparation, Visualization. FX: Methodology, Formal analysis, Supervision. JD: Conceptualization, Validation, Writing—review and editing. YT: Resources, Writing—review and editing.

SUPPLEMENTARY MATERIAL

The Supplementary Material for this article can be found online at: <https://www.frontiersin.org/articles/10.3389/fenrg.2022.875785/full#supplementary-material>

- Lyu, X., Jia, Y., and Dong, Z. (2021). Adaptive Frequency Responsive Control for Wind Farm Considering Wake Interaction. *J. Mod. Power Syst. Clean Energy* 9 (5), 1066–1075. doi:10.35833/MPCE.2020.000237
- Lyu, X., Zhao, J., Jia, Y., Xu, Z., and Wong, K. P. (2019). Coordinated Control Strategies of PMSG-Based Wind Turbine for Smoothing Power Fluctuations. *IEEE Trans. Power Syst.* 34 (1), 391–401. doi:10.1109/TPWRS.2018.2866629
- National Grid ESO. (2019). Technical Report on the Events of 9 August. Available at: <https://www.nationalgrideso.com/document/152346/download> (Accessed September 6, 2019).
- Pérez-Molina, M. J., Larruskain, D. M., López, P. E., and Buigues, G. (2020). Challenges for Protection of Future HVDC Grids. *Front. Energy Res.* 8, 33. doi:10.3389/fenrg.2020.00033
- Prakash, A., Murali, S., Shankar, R., and Bhushan, R. (2019). HVDC Tie-Link Modeling for Restructured AGC Using a Novel Fractional Order cascade Controller. *Electric Power Syst. Res.* 170, 244–258. doi:10.1016/j.epsr.2019.01.021
- Rudez, U., and Mihalic, R. (2011). Monitoring the First Frequency Derivative to Improve Adaptive Underfrequency Load-Shedding Schemes. *IEEE Trans. Power Syst.* 26 (2), 839–846. doi:10.1109/TPWRS.2010.2059715
- Rudez, U., and Mihalic, R. (2016). WAMS-based Underfrequency Load Shedding with Short-Term Frequency Prediction. *IEEE Trans. Power Deliv.* 31 (4), 1912–1920. doi:10.1109/TPWRD.2015.2503734
- Shi, Q. M., Guo, M. Q., Liu, K., Wang, Y., Zou, X., Zou, Q., et al. (2021). Coordinated Frequency Control for UHVDC Considering Inertia Response. *Power Syst. Tech.* 45 (9), 1084–1090. doi:10.13335/j.1000-3673.pst.2021.0015
- Sigrist, L., Egido, I., and Rouco, L. (2012). A Method for the Design of UFLS Schemes of Small Isolated Power Systems. *IEEE Trans. Power Syst.* 27 (2), 951–958. doi:10.1109/TPWRS.2011.2174448
- Skrjanc, T., Mihalic, R., and Rudez, U. (2021). A Non-Intrusive Approach for Enhancing Power-System Frequency Stability. *IEEE Trans. Power Syst.*, 1. doi:10.1109/TPWRS.2021.3131098
- Song, Z. O., Liu, J. Y., Liu, Y., Masoud, B., and Liang, W. (2014). WAMS-based Adaptive UFLS Considering Dynamic Correction. *Electric Power Automation Equipment* 34 (4), 95–100. doi:10.3969/j.issn.1006-6047.2014.04.017
- Terzija, V. V. (2006). Adaptive Underfrequency Load Shedding Based on the Magnitude of the Disturbance Estimation. *IEEE Trans. Power Syst.* 21 (3), 1260–1266. doi:10.1109/TPWRS.2006.879315
- Tian, Z., Xiao, Q.-W., and Ren, F.-R. (2021). Assessing the Efficiency and CO₂ Reduction Performance of China's Regional Wind Power Industry Using an Epsilon-Based Measure Model. *Front. Energy Res.* 9, 672183. doi:10.3389/fenrg.2021.672183
- Tofis, Y., Timotheou, S., and Kyriakides, E. (2017). Minimal Load Shedding Using the Swing Equation. *IEEE Trans. Power Syst.* 32 (3), 2466–2467. doi:10.1109/TPWRS.2016.2614886

- Van de Vyver, J., De Kooning, J. D. M., Meersman, B., Vandeveld, L., and Vandoorn, T. L. (2016). Droop Control as an Alternative Inertial Response Strategy for the Synthetic Inertia on Wind Turbines. *IEEE Trans. Power Syst.* 31 (2), 1129–1138. doi:10.1109/TPWRS.2015.2417758
- Vidyanandan, K. V., and Senroy, N. (2013). Primary Frequency Regulation by Deloaded Wind Turbines Using Variable Droop. *IEEE Trans. Power Syst.* 28 (2), 837–846. doi:10.1109/TPWRS.2012.2208233
- Yang, D. Y., and Cai, G. W. (2016). The Sensitivity of Load Shedding Control and its Application in Wide-Area Low Frequency Protection. *Electric Power Automation Equipment* 36 (3), 124–128. doi:10.16081/j.issn.1006-6047.2016.03.019
- Yang, G. C. (2007). *The Principle of Automatic Power System*. Beijing: China Electric Power Press.
- Ye, H., Pei, W., and Qi, Z. (2016). Analytical Modeling of Inertial and Droop Responses from a Wind Farm for Short-Term Frequency Regulation in Power Systems. *IEEE Trans. Power Syst.* 31 (5), 3414–3423. doi:10.1109/TPWRS.2015.2490342
- Zhao, W. J. (2004). *Technology for HVDC Transmission Project*. Beijing: China Electric Power Press.

Conflict of Interest: Author FX was employed by the NARI Group Corporation (State Grid Electric Power Research Institute).

The remaining authors declare that the research was conducted in the absence of any commercial or financial relationships that could be construed as a potential conflict of interest.

Publisher's Note: All claims expressed in this article are solely those of the authors and do not necessarily represent those of their affiliated organizations, or those of the publisher, the editors and the reviewers. Any product that may be evaluated in this article, or claim that may be made by its manufacturer, is not guaranteed or endorsed by the publisher.

Copyright © 2022 Wu, Xue, Dai and Tang. This is an open-access article distributed under the terms of the Creative Commons Attribution License (CC BY). The use, distribution or reproduction in other forums is permitted, provided the original author(s) and the copyright owner(s) are credited and that the original publication in this journal is cited, in accordance with accepted academic practice. No use, distribution or reproduction is permitted which does not comply with these terms.